Advanced laser based measurements in porous media combustion

M.C. Weikl[1], T. Seeger[1,*],F. Beyrau[2], A. Leipertz[1] and S.A. Tedder[3]

[1] Lehrstuhl für Technische Thermodynamik (LTT), Universität Erlangen-Nürnberg, D-91058 Erlangen, Germany

[2]Now with: Department of Mechanical Engineering, Imperial College London, London, UK

[3]Advanced Sensing and Optical Measurement Branch, NASA Langley Research Center, Hampton, VA, USA

Abstract

We present measurements using dual-pump dual-broadband coherent anti-Stokes Raman scattering spectroscopy (DP-DBB-CARS) inside a porous media burner. This work continues our previous measurements in such combustion systems. The existing setup was significantly modified with the aim of providing improved data quality and data rate, reduction of interferences and additional species information. These changes are presented and discussed in detail.

The CARS technique was expanded to a dual-pump dual-broadband CARS system which in principle enables acquisition of temperatures together with relative H_2/N_2- and O_2/N_2- species concentrations. Experimental complexity was reduced by the use of a modified spectrometer enabling the detection of both signals, vibrational and rotational CARS, with only one detection system.

Introduction

Nowadays combustion of fossil fuels is still the most important source of energy and power. Applications such as gas turbines, internal combustion engines and domestic heating systems are getting increasingly sophisticated. However, further optimization of the existing and development of new forward-looking technologies are needed. High efficiency, marginal pollutant emissions and low fuel consumption are desirable standards for modern combustion devices. The porous burner technology is a modern way of energy conversion with a strong potential to achieve this.

For a further optimization of the existing porous burner technology a detailed understanding of the processes inside the pores is necessary. Therefore the complicated interactions of flow, chemical reactions and heat transfer mechanisms between the gas and solid phase need to be investigated. However, most studies focused only on a numerical analysis of the combustion process in porous media. Zhou and Pereira [1] investigated the influence of the reaction-mechanism complexity on temperature and species distribution as well as exhaust gas pollutants using numerical simulations. Barra and Ellzey [2] investigated the heat transport processes, and Hackert et al. [3] the interaction of combustion and heat transfer. Hanamura and Echigo [4] analyzed the flame stability in terms of flame blow-off, flashback and extinction.

For a better understanding of the combustion process inside this complex system, accurate measurements of different key parameters are required. But studies employing experimental techniques inside the porous structure are rare in literature which can be attributed to the limited accessibility of the porous medium to mechanical probes. In many cases, global data, e.g., flue gas measurements of temperature, NO and CO were conducted in order to obtain data for the validation of numerical models [5, 6]. Bouma and De Goey [7] performed flue gas temperature measurements using coherent anti-Stokes Raman scattering along with infrared pyrometry for determining the surface temperature of a ceramic foam burner. However, the derivation of information about the local processes inside the porous foam from global exhaust gas measurements is certainly limited. Besides this, there are also studies with temperature information from the reaction zone obtained using thermocouples [8, 9]. Due to the strong radiation inside the porous structure and the fact that mechanical contact between the probe and the ceramic cannot be eliminated, the reliability of the measurements is not easy to assess.

In general, optical experimental methods are more appropriate for local combustion studies with high accuracy. However, for the application of conventional optical techniques like spontaneous Raman scattering, laser Rayleigh scattering or laser-induced fluorescence (LIF) the limited optical accessibility is a challenge as normally the signals need to be collected with large numerical apertures. To overcome this problem, coherent optical measurement techniques can be employed since their signal is strong and, even more important, can have a very small numerical aperture. As a result they need merely small optical accesses. For the application described in this work, coherent anti-Stokes Raman scattering (CARS) is a favorable tool, because it can provide temperature as well as species concentration information (see e.g. [10]). Moreover, it is already a well established tool for measurements in

* Corresponding author: ts@ltt.uni-erlangen.de

Associated Web site: http://www.ltt.uni-erlangen.de

Lehrstuhl für Technische Thermodynamik (LTT) & Erlangen Graduate School in Advanced Optical Technologies (SAOT), Friedrich-Alexander Universität Erlangen-Nürnberg, Am Weichselgarten 8, D-91058 Erlangen, Deutschland, phone: +49-9131-85-29776, fax: +49-9131-85-29901

technical systems with limited optical access [11, 12]. In previous work, we have demonstrated first gas phase temperature measurements inside a porous burner to show the potential of this technique [13]. Nevertheless for a more detailed analysis of the combustion process an improved data rate and data quality, reduction of interferences additional species information is helpful. This was achieved here by using a modified DP-DBB-CARS setup. With this setup improved results from a premixed methane/air combustion inside a porous burner were shown.

Experimental approach

A dual-pump CARS setup consists essentially of three lasers, two narrowband and one broadband. One of the narrowband lasers is typically a solid-state laser, i.e., a frequency-doubled Nd:YAG laser (ω_1) with a fixed emission wavelength of 532 nm. The second narrowband laser is commonly a tunable dye laser (ω_2). For the generation of signals from two different molecules the frequency difference of each pump laser and the broadband dye laser (ω_S) has to coincide with the Raman transition of interest. Hence for nitrogen and hydrogen two combinations are possible:

$$\omega_1 - \omega_S = \Delta\omega_{N_2} \quad ; \quad \omega_2 - \omega_S = \Delta\omega_{H_2} \qquad (1)$$

$$\omega_1 - \omega_S = \Delta\omega_{H_2} \quad ; \quad \omega_2 - \omega_S = \Delta\omega_{N_2} \qquad (2)$$

This is shown schematically in the energy diagram in Figure 1

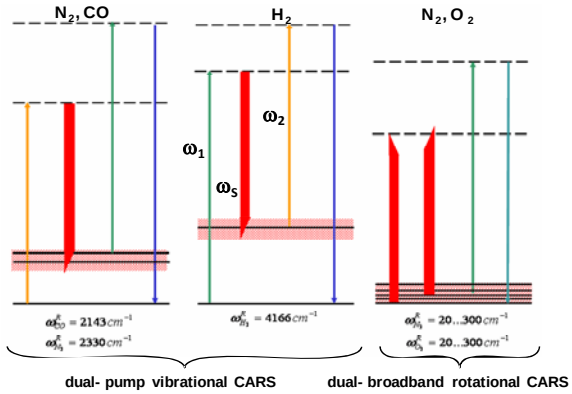

Figure 1: Energy level diagram for the dual-pump dual broadband CARS approach

The frequency-doubled radiation from a Nd:YAG laser provides the pump beams for the CARS process and for the two dye lasers. The Nd:YAG is equipped with a seeder and can thus be operated in single longitudinal mode with a bandwidth of 0.003 cm^{-1}. Part of the laser pulse was split off to pump a narrowband dye laser equipped with an intra-cavity etalon (0.03 cm^{-1}) operated with the laser dye Rhodamine B solved in ethanol. This laser acts as a second pump laser (ω_2). The output was tuned to 593.7 nm to optimize the position of the CARS signal of hydrogen relative to the fixed signal positions of nitrogen and carbon monoxide, i.e., to minimize spectral overlap. With these wavelengths, all the vibrational CARS-signals can be detected in a region between 473 nm and 478 nm. The broadband dye laser output was split into two beams. One is used in the dual-pump CARS process.

Additionally, both broadband beams generate together with the Nd:YAG beam a dual-broadband pure rotational CARS signal as shown in Fig. 1. The polarization of all beams were aligned in vertical direction and controlled with polarizing prisms. Pulse energies in each of the four beams were adjusted to be approximately 20 mJ per pulse. An f=300 mm focal length lens was used to focus the beams in a folded BOXCARS arrangement. To reduce the effect of stray light onto the rotational CARS signal, the ω_1-beam was directed into a beam-dump before the collimating lens (f=300 mm). Due to the folded BOXCARS arrangement, both signals, vibrational and rotational CARS, are emitted almost superimposed and collinear but spatially separated from the other laser beams. With the DP-VCARS part of this setup VCARS signals of N_2, CO, and H_2 are in principle accessible and with the DBB-RCARS part rotational lines of e.g N_2, and O_2, can be detected [14]. Two apertures are used for further stray-light rejection. Finally, the signals are focused to the entrance slit of a spectrometer (f=550 mm, 2400 lines/mm) with a nominal resolution of 0.013 nm. An additional lens (cylindrical, f=50 mm) was placed in front of the entrance slit. The vibrational CARS signal is directed to the output plane of the spectrometer. A second mirror (f=500 mm) is placed in the spectrometer to direct the dual-broadband rotational CARS signal to the output plane. With this mirror the dual-broadband rotational CARS signal can be placed independently from the vibrational CARS signal on the same camera chip. The single-pulse spectra were recorded with a CCD camera (1600x1200 pixel). A knife edge is placed on the camera window to inhibit stray light at low Raman shifts from saturating the chip. By reducing the region of interest (ROI) in the height of the chip to the part where the signals were placed, readout time could be reduced to be able to operate at the repetition rate of the Nd:YAG laser. The CARS setup together with a photograph of spectrometer with the paths of the respective signals is shown in Figure 2.

Additionally, a beam monitoring system was applied [15]. For this purpose, a glass plate is placed after the focusing lens (f = 450 mm). The reflected parts of the laser beams are attenuated using neutral density filters. A standard consumer webcam with the lens removed was mounted on a rail to scan along the focal volume. This system was used to fine-adjust the telescopes in the beams, to improve the beam overlap and thus to maximize the signal level, to investigate coalignment of both probe volumes and to measure the dimensions of the probe volume. The length of the measurement volume was approximately 2 mm and 200 microns in diameter. During the course of the CARS-measurements and for further optimizing CARS signal levels, the glass plate was taken out of the beam path.

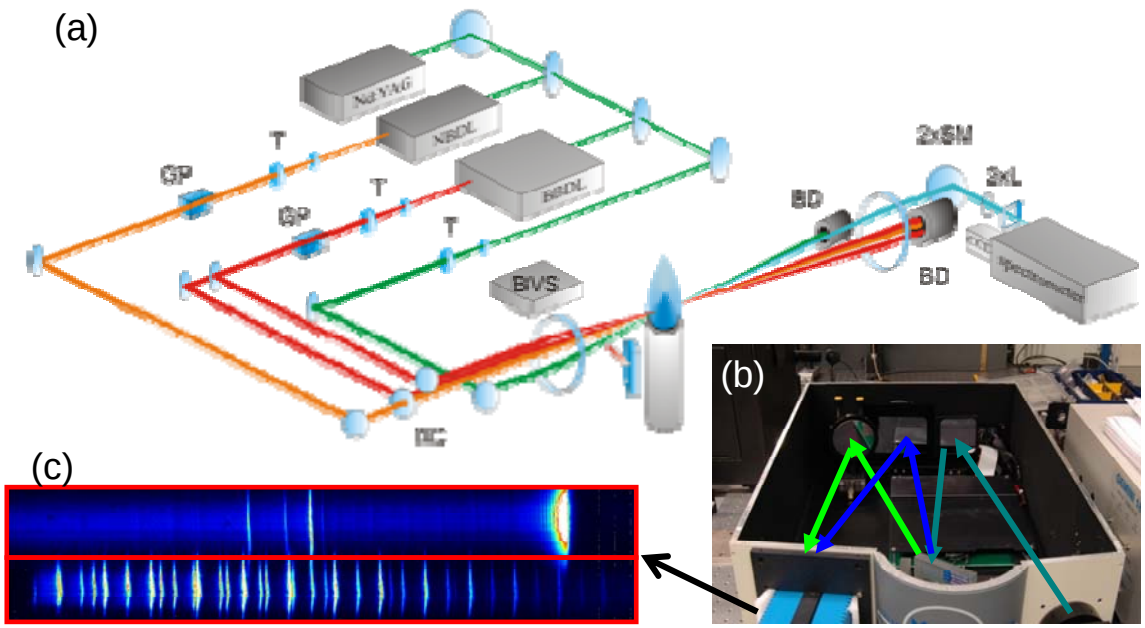

Figure 2: a: Schematic of the experimental DP-DBB-setup with one detection system; T: telescope; GP: Glan-polarizing prisms; BS: beam splitter; DC: dichroic mirror; BVS: beam view system; BD: beam dump; SM: silver mirror; L: lens.
b: Schematic signal traces in the spectrometer – blue/dashed: vibrational-CARS; green/dotted: rotational-CARS.
c: Averaged CCD-image from the spectrometer with region of interest (ROI) for vibrational (top) and rotational CARS signals (bottom)

Rotational CARS signals normally suffer from stray light influence of the narrowband laser source. Therefore a new type of filter with formerly unattained edge steepness was applied in this measurements to realize straylight-free data collection, even in the high scattering area of the porous medium. The performance of the filter is shown in Figure 3 where a comparison of rotational CARS-spectra with and without short pass filter is shown.

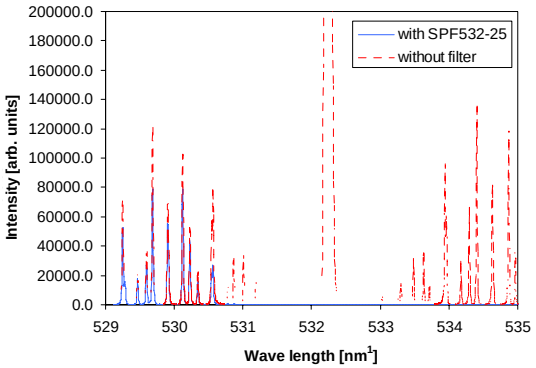

Figure 3: Rotational CARS-spectra with and without the steep short pass filter

A sample image from the CCD-camera with spectra from a partially premixed flame is shown in Figure 2c. The upper part of the images displays the DP-VCARS spectrum with lines of nitrogen and hydrogen. The lower part displays the DBB-RCARS spectrum. The spectra are extracted from the respective signals and evaluated using an in house developed CARS code.

The burner assembly is shown schematically in Fig. 4. Two independent gas supplies for methane and air are connected to a mixing chamber. The individual flow rates are set by mass flow controllers assuring a stoichiometric mixture of fuel and oxidizer. After passing the flame trap consisting of a ceramic plate of 20 mm in thickness with evenly distributed holes (diameter 1.5 mm), the methane/air mixture was ignited within the porous material of a SiC ceramic foam. Further details of the burner can be found elsewhere [13].

In order to facilitate measurements within the porous structure the mixing chamber of the burner was equipped with an anti reflective coated fused silica window allowing optical access. By positioning the burner properly, a position could be found where a line-of-sight access was provided through the flame trap as well as the ceramic foam where the combustion was taking place. The laser beam pathways are indicated in Figure 4. At least the part of the signal that was not obscured by the small aperture of the pores is detected. However, since the CARS signal is comparatively strong, a sufficient

amount of signal was collected and analyzed. The whole burner was mounted to a translation stage so that the probe volume could be moved along a line throughout the entire reaction zone. For this purpose great care was taken to adjust the mechanical components in order to avoid the need for a realignment of the optical system at different probe volume positions.

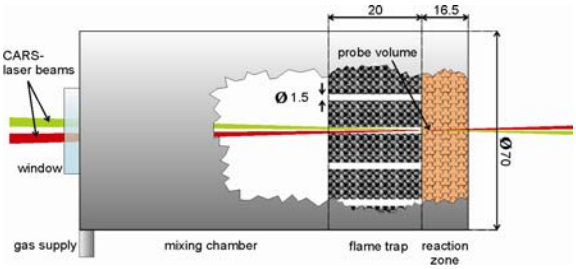

Figure 4: Schematic drawing of the burner assembly: the window providing optical access as well as the CARS laser beam pathways is indicated.

Results and Discussion

The experimental results were obtained with a methane air mixture at ϕ=1.0 resulting in a thermal power density of 259 kW/m^2. Negative values at the spatial axis in the following plots indicate a position inside the flame trap. The ceramic foam in which the combustion takes place is located between x=0mm and x=16.5 mm marked by the dotted line. This operation condition results in a total flow rate of 17.7 sl/min. The initial temperature of the methane/air mixture was 300 K.

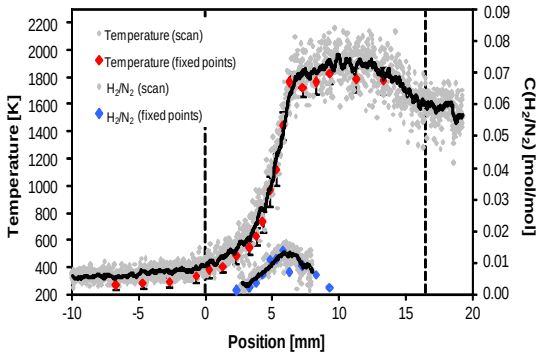

Figure 5: A comparison of scanning and fixed point measurements

In order to enhance the data rate the burner was mounted on an electronic controlled translation stage. A constant movement of 10 mm/min allowed an acquisition of 60 single shot CARS measurements per mm. A comparison of such a scan measurement and point wise measurements of temperature and relative H_2/N_2 concentration is shown in Figure 5. For each fixed point 250 single shot spectra were recorded. In both trends no strong local fluctuations can be seen and hence it can be concluded that the flame front in this case is stationary. By employing these scanning measurements, the data rate is improved and the measurement time for one profile is reduced by 80%. In addition in order to enhance the H_2 accuracy a new linewidth model is implemented in the evaluation code [16].

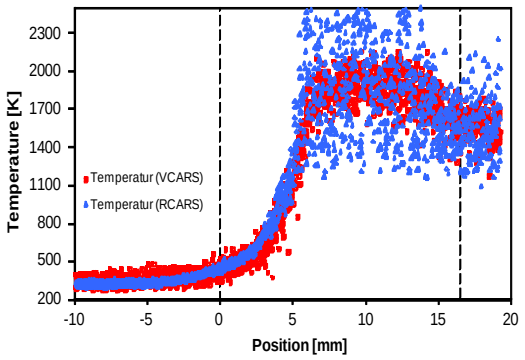

Figure 6: Simultaneous rotational and vibrational CARS temperature scans

With the DP-DBB-CARS system it was possible to measure simultaneously temperatures evaluated from a rotational and a vibrational CARS signal. It is well known that rotational CARS is more precise at low temperatures and vibrational CARS at high temperatures. This can be seen clearly in the temperature scan in Figure 6. Therefore by using both techniques simultaneously the temperature precision can be improved.

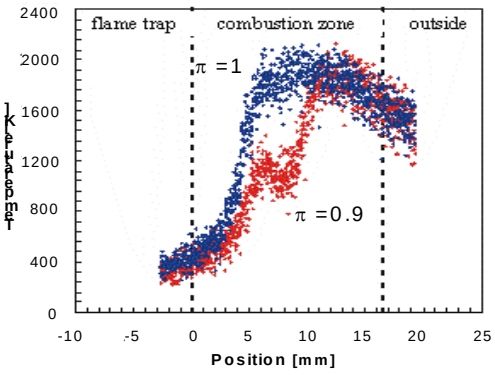

Figure 7: Temperature profiles measured for ϕ=1 and ϕ=0.9

In order to investigate the stability of the flame front position the flow rates and the stochiometry were varied. In Figure 7 temperature profiles are shown for ϕ=1 and ϕ=0.9. The corresponding thermal power density was 1.1 kW and 1.0 kW. The temperature profile in Figure 7 suggests a complex temperature distribution and the need to measure two or three dimensional temperature distributions to

understand this process. This is demonstrated in Figure 8. Here for one pore temperature profiles at different positions perpendicular to the burner axis were taken and by a linear interpolation a two dimensional temperature map was provided. Two different burner conditions were compared. The conditions were ϕ=1 (Fig. 8a) and ϕ=0.8 (Fig. 8b). The corresponding thermal power density was 1 kW and 0.9 kW respectively. It can be seen that the flame front is not perpendicular to the burner axis and a variation of the burner conditions is resulting in strong shifts of the flame front position. The flame front in Figure 8b is located between 10-12 mm downstream. But already a first temperature increase at about 7 mm downstream could be observed. A reason for this can be a small gas flow perpendicular to the burner axis. This can be verified by further concentration measurements e.g. of oxidizer and fuel.

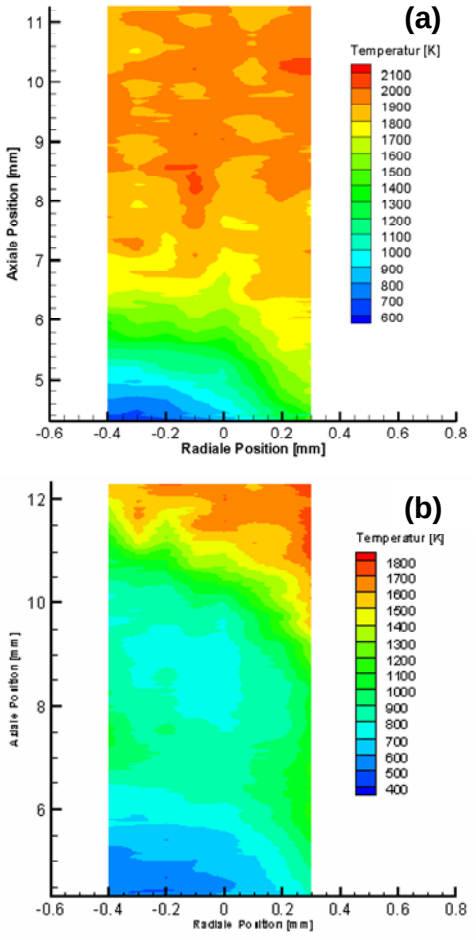

Figure 8: Two dimensional temperature maps provided a linear interpolation of temperature profiles at different positions perpendicular to the burner axis for ϕ=1 (a) and ϕ=0.8 (b)

Summary and conclusions

Improved laser-based measurements of the gas phase temperature within a porous burner were conducted. With a modified setup an improved data quality and data rate, and additional species information were achieved. The measurements reveal the complex flame shape, probably determined by the foam geometry This demonstrates the necessity to receive experimentally two or three dimensional temperature and concentration fields to understand the complex combustion process inside the porous foam.

Acknowledgement

The authors gratefully acknowledge financial support for parts of the work by the German Science Foundation DFG and for funding the Erlangen Graduate School in Advanced Optical Technologies (SAOT) within the framework of the German Excellence Initiative.

The authors gratefully acknowledge the supply of the burner by the Lehrstuhl für Strömungsmechanik LSTM in Erlangen.

References

[1] X.Y. Zhou, J.C.F. Pereira, Fire and Materials 22 (1998) 187-197.
[2] A.J. Barra, J.L. Ellzey, Combust. Flame 137 (2004) 230-241.
[3] C.L. Hackert, J.L. Ellzey, O.A. Ezekoye, Combust. Flame 116 (1999) 177-191.
[4] K. Hanamura, R. Echigo, Wärme- und Stoffübertragung 26 (1991) 377-383.
[5] J.R. Howell, M.J. Hall, J.L. Ellzey, Prog. Energy Combust. Sci. 22 (1996) 121-145.
[6] D.J. Diamantis, E. Mastorakos, D.A. Goussis, Combust. Theory Model. 6 (2002) 383-411.
[7] P.H. Bouma, L.P.H. De Goey, Combust. Flame 119 (1999) 133-143.
[8] D.K. Min, H.D. Shin, Int. J. Heat Mass Transf. 34 (1991) 341-356.
[9] G. Brenner, K. Pickenäcker, O. Pickenäcker, D. Trimis, K. Wawrzinek, T. Weber, Combust. Flame 123 (2000) 201-213.
[10] A.C. Eckbreth, Laser Diagnostics for Combustion Temperature and Species, 2nd ed., Gordon and Breach, 1996.
[11] M.C. Weikl, F. Beyrau, A. Leipertz, Appl. Opt. 45 (2006) 3646-3651.
[12] A. Braeuer, F. Beyrau, M.C. Weikl, T. Seeger, J. Kiefer, A. Leipertz, A. Holzwarth, A. Soika, Journal of Raman Spectroscopy 37 (2006) 633-640.
[13] J. Kiefer, M. C. Weikl, T. Seeger, F. von Issendorff, F. Beyrau, A. Leipertz, Proc. of the Combust. Inst. 32 (2009) 3123-3129

[14] M. C. Weikl, Y. Cong, T. Seeger, A. Leipertz, Appl. Opt. 48 (2009) B43-B50
[15] S. A. Tedder, M. C. Weikl, T. Seeger, A. Leipertz, Appl. Opt. 47 (2008) 6601-6605
[16] Y. Gao, M. C. Weikl, T. Seeger , A. Leipertz, P. Joubert, J. Bonamy, accepted by Journal of Raman Spectroscopy (2009)